Cooperative Control of Drive Motor and Clutch for Gear Shift of Hybrid Electric Vehicles with Dual-clutch Transmission

Sooyoung Kim and Seibum B. Choi, *Member, IEEE*

***Abstract*—This study deals with cooperative control of drive motor and clutches for the gear shift of a parallel hybrid electric vehicle (HEV) with dual-clutch transmission (DCT). A HEV with DCT powertrain requires sophisticated control of two clutch actuators and power sources to achieve outstanding gear shift performances. In this work, a new shift control strategy based on the feedback of both speed and torque states is implemented to improve the shift quality. Differently from previous approaches, the proposed control uses the dynamic torque observer to accurately track the desired transient torque during the inertia phase. Since a drive motor is installed in the HEV's driveline, the transient torque through the driveline can be effectively controlled by using the fast dynamic characteristics of the drive motor. A major difficulty arising from the shift control of DCT is the interactions between the speed and torque control loops. To treat the coupling effects effectively even in the presence of model uncertainties and disturbances, a robust multivariable control scheme using H-infinity loop shaping is suggested especially for the inertia phase control. The performance of the final observer-based controller is demonstrated through real time experiments. Comparative study with the conventional control approach is also conducted, and detailed discussions of the results are provided.**

***Index Terms*—Dual-clutch transmission, Hybrid electric vehicle, Gear shift control, Robust multivariable control, Torque control**

NOMENCLATURE

c_o Torsional damping coefficient of output shaft.

i_{t1} Gear ratio of input and transfer shaft 1.

i_{t2} Gear ratio of input and transfer shaft 2.

i_{f1} Final reduction gear ratio 1.

i_{f2} Final reduction gear ratio 2.

J_{in} Equivalent inertia of power sources.

$J_{ct2,eq}$ Equivalent inertia of transmission part seen from output shaft.

J_v Vehicle inertia.

k_o Torsional stiffness of output shaft.

T_{c1} Clutch 1 torque.

T_{c2} Clutch 2 torque.

T_{in} Torque from power sources.

T_o Output shaft torque.

T_v Vehicle resistance torque.

ω_{c1} Clutch 1 speed (input shaft 1 speed).

ω_{c2} Clutch 2 speed (input shaft 2 speed).

ω_{in} Speed of power sources (for parallel mode operation).

ω_w Wheel speed.

I. INTRODUCTION

HYBRID electric vehicles (HEVs) provide lower emissions and better fuel economy than conventional engine-driven vehicles by effectively using dual energy sources, a fuel and electrical energy. Managing the power distribution between the two sources and determining the optimal gear ratio in any driving conditions are crucial to improve the performance of HEVs. The typical objective of such power management control strategies is to minimize fuel consumption while satisfying the driver's power demand and other constraints such as emissions, drivability, and regulation of state of charge. Previously, various power management strategies were proposed to optimize fuel economy and emissions of HEVs in different configurations [1-7].

The power management control provides set-points for individual servo control loops that operate at a much higher frequency. In order to attain the optimized HEV performance designed by the power management strategy, each servo control loop should reliably achieve the corresponding set-point. Among the servo control loops, control of the transmission system is, in particular, important to perform the actual gear

S. Kim is with Hyundai Motor Company, Hwasung 18280, South Korea (e-mail: westkllr@kaist.ac.kr). S. B. Choi is with the Department of mechanical engineering, KAIST, Daejeon 34141, South Korea (e-mail: sbchoi@kaist.ac.kr).

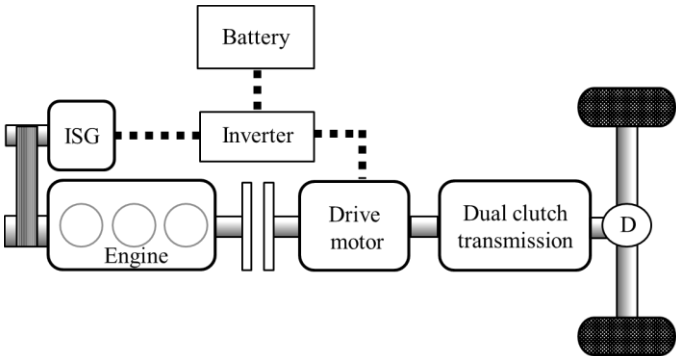

Fig. 1. Configuration of a parallel HEV

shifting for the optimal gear ratio commanded by the power management control loop. In order to attain the best fuel economy during gear shifting, the shift transient time should be minimized so that the optimal gear ratio is achieved as swiftly as possible. However, if the gear shift is performed too quickly, large torque oscillations may occur through the driveline.

The study deals with gear shift control of a parallel-type HEV equipped with a dry dual-clutch transmission (DCT), whose structure is schematically illustrated in Fig. 1. The integrated starter generator (ISG) is connected to the engine via a belt, and is used for engine start. The engine clutch installed between the engine and the drive motor begins to be engaged when the mode transition from pure electric vehicle mode to parallel hybrid mode is required. DCTs use two sets of clutches and transfer shafts during gear shifts to transmit the torque delivered by power sources to the wheel without using torque converters, which can effectively overcome the drawbacks of other types of transmissions. Recently, recognizing its merits, DCT has been applied not only to production HEVs but also to pure electric vehicles [8-11]. However, since there is no smoothing effect of torque converters, DCT powertrains are likely to cause an awkward shift shock during gear shifting, especially when the shifting is performed quickly [12, 13]. Fast gear shifting is generally required to achieve good fuel economy and minimize vehicle acceleration losses, regardless of the type of transmission. In addition, if the driver wants fast acceleration by pressing the accelerator pedal suddenly, the shift time must be shortened accordingly [14]. Smooth and fast shifting conditions are in conflict with each other and are generally regarded as two main goals of shift control [15]. A practical gear shift control strategy should be designed for real vehicle applications, upon consideration of such conflicts among different shift quality criteria.

In general, a gear shift control to achieve the desired gear ratio commanded by the power management strategy consists of two levels: upper-level control that calculates the reference torque values of power sources and clutches satisfying the desired shifting performances, and lower-level control that manages the strategies for each actuator to track the reference torque trajectories. For good control performances, both control loops should be designed together carefully. In [16], the authors proposed a dual-loop self-learning fuzzy controller for the gear engagement control, and experimentally validated the excellence of the developed dual-loop control structure. In specific, the upper-level control deals with the desired shift performance reflected by the driver's accelerator pedal position in the vehicle level; that is, the shift should be performed as fast as the driver wants, and the shift shock should be minimized for driving comfort. In order to achieve these requirements, numerous previous studies have proposed various speed feedback control strategies for the clutch engagement during gear shift [17-19]. Speed-based control has the advantage that no additional sensors are required for production vehicles, and is very effective especially for ATs where damping characteristics of the torque converter exist. However, DCTs require more elaborate control of clutches and power sources focusing on shift shock minimization, although the clutch-to-clutch shifting process is analogous to that of ATs [14, 19]. For sophisticated control of DCT, integrated torque and speed controllers for DCTs were proposed in [15, 20-22]. The authors made use of calculated static torque values based on the driveline model equations to deal with the absence of torque sensors. In [23-25], various methods were proposed to estimate the transient torque through DCT drivelines more accurately, but how to actually use them in real-time gear shift controls has not been dealt with.

In this work, an output shaft torque based shift control strategy is proposed to improve the gear shift performance of a parallel HEV with DCT. Differently from previous studies, this work tries to achieve the desired shift performance through simultaneous tracking control of dynamic output torque and speed states during the shift transient. Also, since the drive motor provides more accurate and faster torque control compared with the engine, the motor will be mainly utilized for the gear shift control. Here, the output shaft torque and the slip speed of the on-coming clutch are selected as the outputs to be controlled by the three actuators: the off-going clutch, the on-coming clutch, and the power source (drive motor). The gear shift control problem is then interpreted as the tracking control problem of the speed and the torque states in the vehicle driveline. Another important issue arising in the shift control is the strong interactions between the speed control loop and torque control loop. Hence, a robust multivariable controller is designed as the upper-level control to treat the coupling effects effectively, in spite of the presence of model uncertainties and disturbances. The lower-level torque tracking controller for individual clutch actuators is also implemented to be coordinated with the upper-level controller, considering the actuator dynamics.

This paper is organized as follows. In Section II, a driveline model for a parallel HEV with dry DCT is introduced, and the design procedure of the driveline torque observer is presented. The torque observer will be used for the shift control in replace with torque sensors. In Section III, the detailed design procedure of the new gear shift controller is described. The theory and philosophy behind the proposed control strategy are also explained. In Section IV, the control performance of the proposed gear shift controller is evaluated through real-time experiments. Finally, this work is concluded in Section V.

II. Driveline Modeling and Torque Estimation

A. Driveline Model

Differently from the conventional engine-driven vehicle, the parallel HEV dealt with in this work has two additional electric machines: an ISG and a drive motor [26]. Since this work is interested in gear shift control of a HEV, we only consider its parallel mode operations where the engine clutch is engaged and thus the vehicle is partially or fully driven by the engine. For detailed information on all the operation modes of a parallel HEV, see [26, 27]. Then, the driveline structure can be simply described by the third order dynamics, as illustrated in Fig. 2. Next, we define slip speed of on-coming clutch (clutch 2), torsion rate of output shaft, output shaft torque as three states $x_1,\ x_2,\ x_3$, i.e. $x_1=\omega_{in}-\omega_{c2},\ x_2=\dfrac{\omega_{c2}}{i_{t2}i_{f2}}-\omega_w,\ x_3=T_o$.

x_1 stands for the slip speed between the drive motor (or power sources) and the oncoming clutch (clutch 2). In general, x_1 and x_3 are considered as control outputs of a gear shifting control system, since the control performance of those states determines the shift quality. Then, the dynamics of the HEV driveline operating in parallel mode is described as follows:

$$\dot{\mathbf{x}}=\mathbf{A}\mathbf{x}+\mathbf{B}\mathbf{u}+\mathbf{E}\delta \quad \text{where}$$

$$\mathbf{x}=(x_1,\ x_2,\ x_3),\ \mathbf{u}=(T_{in},\ T_{c1},\ T_{c2}),\ \delta=T_v$$

$$\mathbf{A}=\begin{bmatrix} 0 & 0 & \dfrac{1}{J_{ct2,eq}} \\ 0 & 0 & -\left(\dfrac{1}{i_{t2}i_{f2}J_{ct2,eq}}+\dfrac{1}{J_v}\right) \\ 0 & k_o & -c_o\left(\dfrac{1}{i_{t2}i_{f2}J_{ct2,eq}}+\dfrac{1}{J_v}\right)\end{bmatrix},\mathbf{E}=\begin{bmatrix}0\\ \dfrac{1}{J_v}\\ \dfrac{c_o}{J_v}\end{bmatrix}$$

$$\mathbf{B}=\begin{bmatrix} \dfrac{1}{J_{in}} & -\left(\dfrac{1}{J_{in}}+\dfrac{i_{t1}i_{f1}}{J_{ct2,eq}}\right) & -\left(\dfrac{1}{J_{in}}+\dfrac{i_{t2}i_{f2}}{J_{ct2,eq}}\right) \\ 0 & \dfrac{i_{t1}i_{f1}}{i_{t2}i_{f2}J_{ct2,eq}} & \dfrac{1}{J_{ct2,eq}} \\ 0 & \dfrac{c_o i_{t1}i_{f1}}{i_{t2}i_{f2}J_{ct2,eq}} & \dfrac{c_o}{J_{ct2,eq}}\end{bmatrix}. \tag{1}$$

Here, input torque from power sources T_{in} is defined by the sum of torques from all the power sources, i.e. $T_{in} \square i_{ISG}T_{ISG}+T_e+T_{dm}$ where i_{ISG} is gear ratio between ISG and engine, and T_{ISG}, T_e, T_{dm} are torques produced by ISG, engine, drive motor, respectively.

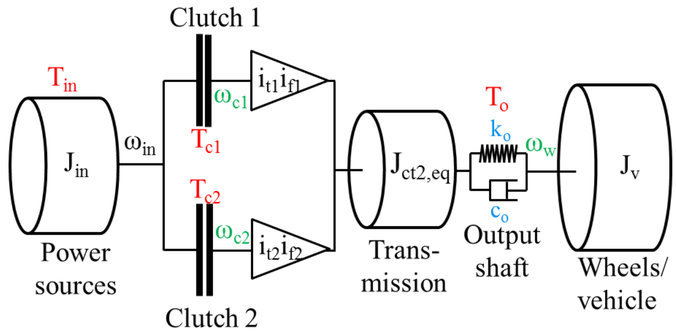

Fig. 2. Driveline model structure

B. Torque Observer Design

One major difficulty arising in the gear shift control is the absence of torque sensors in production vehicles, even though knowledge of torque states of the driveline is essential for the accurate control. Thus, an observer to concurrently estimate transient torque through individual clutches and output shaft is designed in this sub-section.

First, using (1), a linear state observer is developed to estimate the output shaft torque, as follows:

$$\dot{\hat{\mathbf{x}}}=\mathbf{A}\hat{\mathbf{x}}+\mathbf{B}\hat{\mathbf{u}}+\mathbf{E}\delta+\mathbf{L}\mathbf{C}\tilde{\mathbf{x}}$$

$$\text{where } \hat{\mathbf{x}}=(\hat{x}_1,\ \hat{x}_2,\ \hat{x}_3)^T,\ \hat{\mathbf{u}}=(T_{in},\ \hat{T}_{c1},\ \hat{T}_{c2})^T,\ \delta=T_v \tag{2}$$

$$\mathbf{C}=\begin{bmatrix}1&0&0\\0&1&0\end{bmatrix},\ \mathbf{L}=\begin{bmatrix}L_{11}&L_{12}\\L_{21}&L_{22}\\L_{31}&L_{32}\end{bmatrix},\ \tilde{\mathbf{x}}=\mathbf{x}-\hat{\mathbf{x}}$$

Here, $\mathbf{L}$ is the observer gain matrix.

The vehicle load torque can be estimated by combining the net input torque multiplied by gear ratios and the whole vehicle inertia, as follows:

$$T_v=i_t i_f T_{in}-J_{v,eq}\dot{\omega}_w, \tag{3}$$

where i_t, i_f is the current gear ratio and $J_{v,eq}$ is the equivalent vehicle inertia from wheel perspective when one of the clutches is engaged with the flywheel. It is worth noting that the equation (3) is valid if one of the clutches is engaged and the other one is disengaged. Thus, the equation (3) is applicable to general driving conditions except for the short durations of gear shifts and vehicle launch. Under the assumption that the vehicle load does not change during the vehicle launch and each gear shift, equation (3) is used in the torque observer design.

In fact, torque estimation merely based on (2) may not exhibit good accuracy because the individual clutch torque values, i.e. T_{c1}, T_{c2} cannot be modelled accurately. To resolve the problem, the equation (4) for modelling torque transmitted through a clutch during slipping is considered.

$$T_c=\mu_k r_c N F_n, \tag{4}$$

where μ_k, F_n, r_c, and N are the kinetic friction coefficient, and actuator normal force, effective torque radius, and number of friction surfaces of the clutch. Because the parameters in (4) such as the kinetic friction coefficient change continuously with the slip rate of the clutch and environmental factors such as temperature, the clutch torque model is expressed as (5) by dividing it into known and unknown parts:

$$T_c = \left(\mu_{k,n} f_n + \varepsilon_c\right) r_c N \theta_m, \quad (5)$$

where $\mu_{k,n}$, f_n are nominal values of dynamic friction coefficient and a constant determining the relation between clutch normal force F_n and clutch actuator stroke θ_m. Also, ε_c is the uncertain part of the parameters that needs to be identified. The adaptation laws for individual clutch torques are designed to estimate the clutch torque parameters, as follows [32]:

$$\dot{\hat{\varepsilon}}_{c1} = L_{c1}\left(-\left(\frac{1}{J_{in}} + \frac{i_{t1} i_{f1}}{J_{ct2,eq}}\right)\tilde{x}_1 + \frac{i_{t1} i_{f1}}{i_{t2} i_{f2} J_{ct2,eq}}\tilde{x}_2\right) r_{c1} N_1 \theta_{m1}, \quad (6)$$

$$\dot{\hat{\varepsilon}}_{c2} = L_{c2}\left(-\left(\frac{1}{J_{in}} + \frac{i_{t2} i_{f2}}{J_{ct2,eq}}\right)\tilde{x}_1 + \frac{1}{J_{ct2,eq}}\tilde{x}_2\right) r_{c2} N_2 \theta_{m2}. \quad (7)$$

The adaptation laws have a role to correct the parameter values based on the feedback of the errors between the linear state observer's responses and the measured ones, $\tilde{x}_1$, $\tilde{x}_2$. Using the adaptive torque observer (combining (2) with (6) and (7)), torque values through each clutch and output shaft during a gear shift can be estimated, and the estimated torque information will be directly used for implementing the shifting controller designed in the next section. In fact, even though we tried to treat parametric uncertainties of clutch using the adaptive torque observer for practical control purposes in this paper, the influences of temperature field and slipping speed on the torque transmissibility should be handled by accurate modeling of the physical phenomena, ultimately. For more information, see [28-31].

III. Control Strategy Development

A. Overview

In this section, a novel control strategy is proposed for gear shifts of a parallel HEV with dry DCT. The control strategy is developed for the 1-2 upshift, which is difficult to control due to the large amount of torque transmission. The goal of the DCT shift control is to perform the clutch-to-clutch shift as fast as the driver's intention while satisfying the criteria of shift smoothness and drivability. A gear shift process of a DCT is usually discriminated as two phases: torque phase where the torque handover from the off-going clutch to the on-coming one occurs and inertia phase where the on-coming clutch with a new gear ratio is synchronized with the power sources. However, in this study, we consider the end phase additionally, which comes immediately after the inertia phase, for more accurate driveline oscillation control. Specifically, in the case of the HEV, the drive motor can be used for reducing driveline oscillations during the end phase. Different control strategies will be developed for each phase in the following sub-sections.

The proposed control uses the dynamic torque observer to accurately track the desired transient torque as well as the clutch slip speed during the inertia phase to attain smooth and fast shifting. Conventionally, the engine control is limitedly used in gear shifts due to the slow dynamics of the engine. In the case of the HEV, by using the fast dynamic characteristics of the drive motor, one can control the transient torque through the vehicle driveline more effectively than when using engine control only. The feasibility of the drive motor control in mode transition or gear shifts of parallel hybrid cars has been validated in many studies [9, 27, 33, 34]. In addition, the regenerative operation of the motor makes the gear shift process more efficient. A robust multivariable controller is developed for coordinated control of the drive motor and the on-coming clutch especially during the inertia phase that dominantly determines the whole shift quality. The control strategies for each shift phase are summarized in Table I.

B. Gear Shift Process Analysis

Figure 3 illustrates typical responses of a DCT vehicle during gear shifting from 1st to 2nd gear. During the torque phase, the off-going clutch stroke is gradually decreased while the on-coming clutch stroke is increased so that torque handover from the off-going clutch to the on-coming one is performed.

TABLE I
Control Strategy for Each Shifting Phase

	Torque phase	Inertia phase	End phase
Controller type	Open-loop	Closed-loop	Closed-loop
Control objective	Disengagement of off-going clutch & engagement of on-coming clutch at the right time using torque observer	Multivariable feedback control of output torque and slip speed to ensure fast and smooth shift	Feedback control of drive motor speed to minimize lock-up oscillation

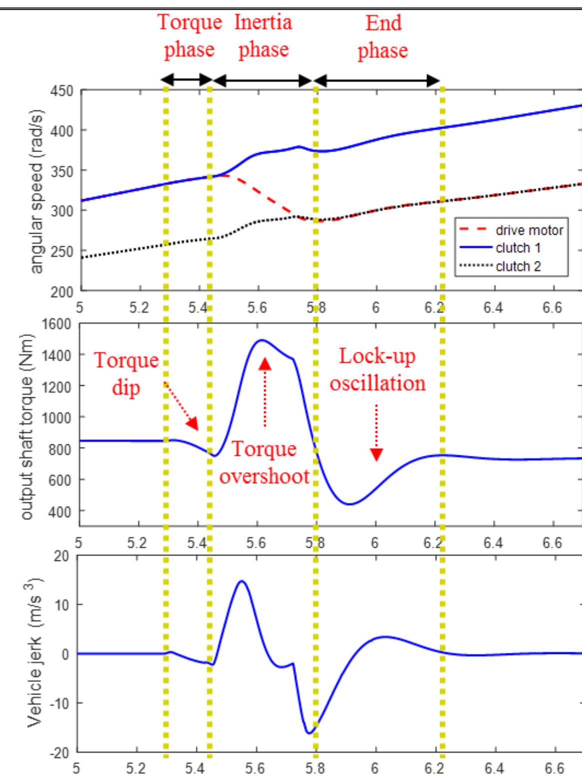

Fig. 3: Typical responses of a vehicle with DCT during an upshift

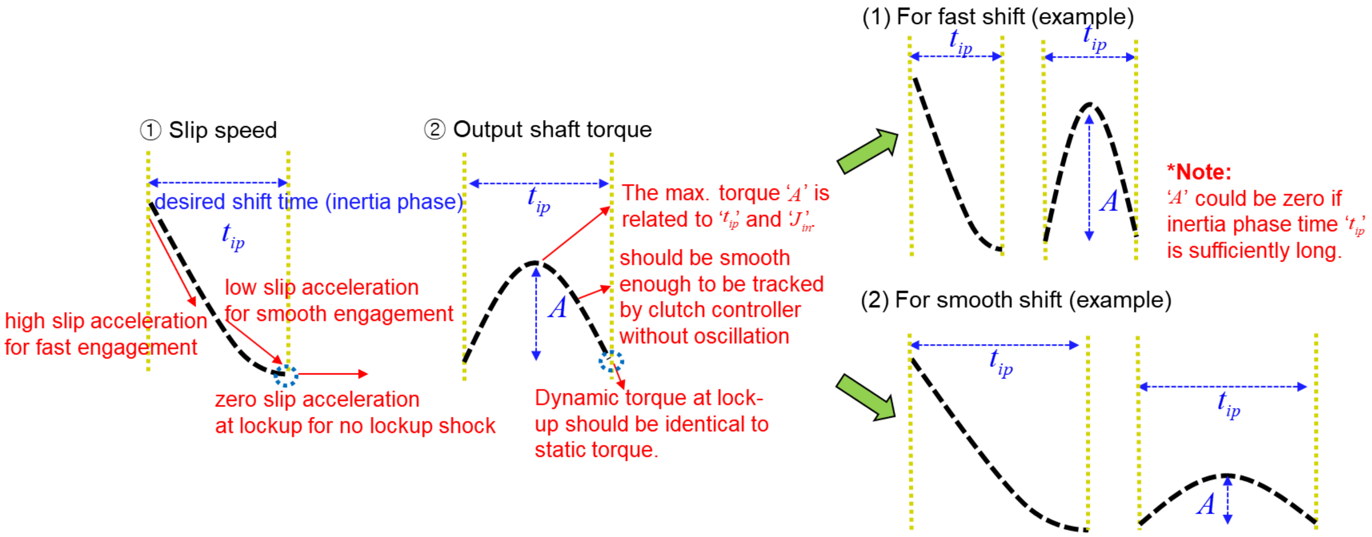

Fig. 4. Desired state trajectories with the proposed control strategy

In this phase, the output torque is somewhat reduced due to the gear ratio change. Note that even if the disengagement of the off-going clutch and the engagement of the on-coming clutch are optimally controlled, output torque dip is unavoidable unless the power source torque is further increased. As soon as the off-going clutch starts to slip, the inertia phase immediately begins. During the inertia phase, the speed or power of the power sources should be reduced to be synchronized with the input shaft with a new gear ratio. Speed reduction of the engine and all the components mechanically connected to it such as the drive motor and ISG causes large overshoot of the output shaft torque, which deteriorates the shift quality. In the HEVs, the regenerative operation of the drive motor can be used for the inertia torque compensation.

As the on-coming clutch is fully engaged with the drive motor, the end phase begins. The lock-up of the on-coming clutch often accompanies driveline oscillations. The lock-up oscillations are primarily caused by the difference between the dynamic torque of the clutch before the lock-up and its static torque after the lock-up. As shown in Fig. 3, accurate control of the clutch and power sources in the inertia phase and end phase is crucial because relatively large driveline oscillations occur in those phases compared with the torque phase in which there is not much variation of speed or torque. Finding a way to reduce the oscillations that occur after the torque phase without lengthening the shift time is a key to improving the shift performance. As mentioned earlier, many previous studies on the gear shift control have developed speed-based feedback control strategies. However, control based only on the speed information cannot guarantee the best shift smoothness, because the output torque response can be varied according to input combinations of clutch and power sources while maintaining the same slip speed response.

C. Torque Phase Control

The objective of torque phase control is to disengage the off-going clutch and engage the on-coming clutch at the right time without clutch tie-up and engine flare for good drivability. In some previously published studies, the off-going clutch was controlled based on the feedback information of its slip speed to maintain a small amount of slip speed during the torque phase (e.g. [14]). However, in this work, an open-loop control strategy is adopted to avoid the adverse effects of stick-slip vibrations possibly caused by inappropriate feedback control. Using the torque information provided by the observer in real time, the off-going clutch is disengaged at the right time when the torque transmitted through it becomes zero so that driveline oscillations and torque interruptions are minimized [35, 36].

D. Inertia Phase Control

At the very beginning of the inertia phase, the off-going clutch is still slipping and transmits a small part of the torque delivered by the power sources. However, the amount of the off-going clutch torque is much less than that of the on-coming clutch, and thus it can be assumed that the torque transmitted through the off-going clutch during the inertia phase is negligible, i.e. $T_{c1} \approx 0$.

In the inertia phase, cooperative control of the on-coming clutch and the power sources is crucial to ensure fast and smooth clutch engagement with a new gear ratio. The torque control of power sources is necessary to compensate the large inertia torque and the driveline oscillations caused by the abrupt gear ratio change. A robust multivariable feedback controller based on (1) is designed to concurrently control the output shaft torque and the slip speed of the on-coming clutch.

From the analysis in sub-section B, it is inferred that the clutch torque dominantly determines the output torque response during inertia phase, while both clutch torque and power sources torque affect the slip speed response. This indicates the necessity of the simultaneous torque and speed control. In fact, in the conventional engine-driven vehicles, because the engine dynamics is much slower than that of the clutch actuator, decentralized control methods were often used for control and they cannot consider the strong interactions between the torque and speed control loops. However, in HEVs, the usage of the drive motor may increase the whole control performance.

Next, the following three assumptions for the inertia phase control strategy are used:

A1. ISG is not used during gear shifts, i.e. $T_{ISG} = 0$.

A2. To avoid severe torsional distortion through the driveline, the torque reduction of the power sources is limited by the following inequality: $T_{in} = i_{ISG} T_{ISG} + T_e + T_{dm} = T_e + T_{dm} \geq 0$.

A3. As long as the motor power is allowed, the demanded torque reduction for the inertia phase control is only handled by the drive motor.

The third assumption indicates that in order to improve fuel efficiency, the regenerative operation of the motor should be used to compensate for the inertia torque as much as possible without the aid of engine control. It should be noted that the torque reduction control of the engine is inevitably required in addition to the regenerative operation of the drive motor when a gear shift is initiated at a very high speed range of the motor, for example, 6000rpm or more.

1) Desired State Trajectories

Since the control states are directly related to the shift quality, how their reference trajectories are defined is very crucial. Assuming the input torque from power sources is not changed substantially before and after the gear shift, the output shaft torque value right after the lock-up of the on-coming clutch (end of the gear shift) is accurately calculated using the information of the input torque and gear ratio values. If the torque phase control is properly conducted, the initial and end values of the output torque in inertia phase are the same as the value of the static torque obtained when engaged with the new gear. It is necessary to make the desired transient trajectories for the states between the initial and end values in the inertia phase. Given a desired shift time determined by the driver's pedal position, the desired values of the two control states are shaped to enhance the shift smoothness as much as possible. First, we designed the reference shape of the on-coming clutch slip speed such that the magnitude of its deceleration increases from the initial deceleration value until the first half of the inertia phase to reduce the shift time and then decreases until the end of the inertia phase for good ride quality. Most importantly, at the end of the inertia phase, the slip acceleration should be zero to minimize the torque discontinuity between before and after the lock-up [36]. The final value conditions of the slip speed and its acceleration are described as (8):

$$\omega_{sl2}(t_{ip,f}) = \dot{\omega}_{sl2}(t_{ip,f}) = 0, \tag{8}$$

where $t_{ip,f}$ is the end time of the inertia phase. Also, the output shaft torque values should increase until half of the inertia phase for fast engagement and decrease during the other half to minimize the lock-up oscillations. Specifically, by defining T_{o,s_2nd} as the static output torque value when the new gear is engaged after lock-up, the initial and final value conditions for output shaft torque are described as follows:

$$T_o(t_{ip,i}) = T_o(t_{ip,f}) = T_{o,s\_2nd}, \tag{9}$$

where $t_{ip,i}$ is the initiation time of the inertia phase.

The combination of (8) and (9) can ensure minimization of the driveline oscillations after the lock-up. The condition (9) indicates that even though the on-coming clutch stroke is increased at the beginning of inertia phase, the stroke should be decreased again to the level of the next static torque at the lock-up. The desired state trajectories for the states satisfying the desired shift time and boundary conditions (8) and (9) are designed in the form of look-up tables. A sinusoidal shape is adopted to shape the trajectories, which is smooth enough to be tracked by the lower-level actuator controls. As soon as the inertia phase flag is switched-on, the desired value generator operates in real-time to generate the reference values for the inertia phase control. In accordance with the driver's pedal position, the desired shift time and the maximum allowable value of the output torque (denoted as 'A' in Fig. 4) are determined, and the corresponding desired values are given to the controller. Note that the initial output torque value cannot be measured, and thus it is obtained from the torque observer developed in the previous section.

2) Multivariable Feedback Control Law

In this sub-section, a robust multivariable controller as the upper-level control for the driveline states is designed to track the desired state values accurately in the presence of the loop interactions. The upper-level control provides the torque commands for the drive motor and the on-coming clutch. The actuator-level controllers (lower-level control) then conduct torque tracking control to generate the desired torques considering the actuators' characteristics. In specific, the drive motor torque is controlled by the inverter drive through pulse width modulation method, and the clutch actuator is controlled using a simple PD position tracking algorithm to generate the commanded clutch torque.

The robust multivariable controller designed in this paper is an H-infinity loop shaping controller, which is based on H-infinity robust stabilization combined with classical loop shaping [38-40]. The H-infinity loop shaping design procedure is divided into stages: first, the open-loop transfer function matrix of the system is augmented by the pre-compensator to shape its singular values as desired, and second, the shaped transfer function is robustly stabilized with respect to the plant uncertainties (in the form of coprime factor uncertainty) based on H-infinity optimization theory. The main advantage using this approach is that one can easily tune the control performance by shaping the open-loop response based on the knowledge of basic loop shaping. In addition, the H-infinity robust stabilization does not require time consuming iterations to obtain its solution, and explicit formulas for the resulting controller exist, differently from other H-infinity optimization problems.

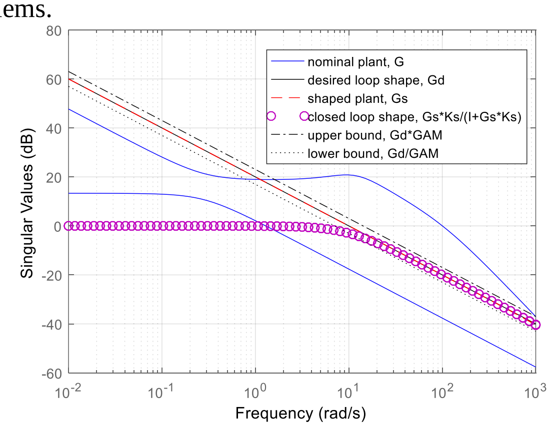

Fig. 5. Results of the singular value shaping

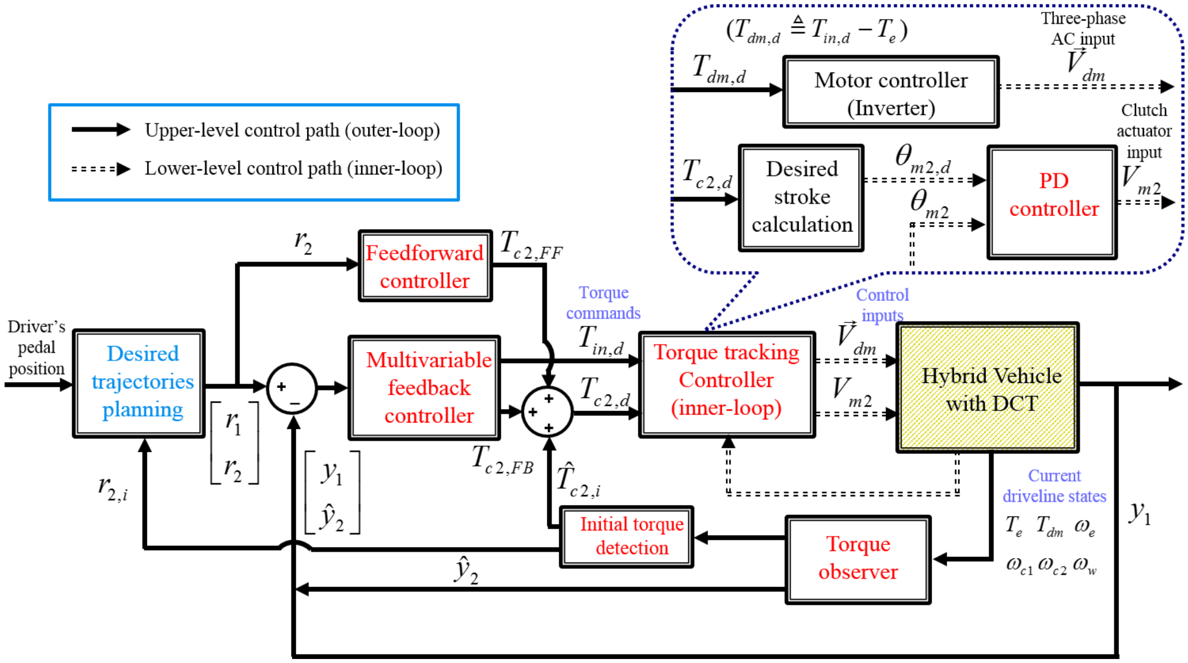

Fig. 6. Inertia phase control structure: observer-based multivariable feedback control + feedforward control

The 2 by 2 transfer function matrix for the DCT driveline is easily obtained using (1) by regarding the vehicle load torque as the disturbance input to the system and assuming $T_{c1} \approx 0$ during inertia phase. When the nominal transfer function matrix is denoted as G, we need to design the prefilter W such that the singular values of the shaped plant $G_s = WG$ is properly determined. In general, the minimum singular value of the loop shape should be large for disturbance rejection and good reference tracking, especially in the low frequency region, while the maximum singular value should be small enough to attenuate the noises in the high frequency region.

In this work, we set the desired loop shape as the pure integral with the gain crossover frequency of 10 rad/s, i.e. $G_d = 10/s$. The desired gain crossover frequency is the main tuning parameter in the loop shaping since it determines the control bandwidth of the closed-loop system. Based on the experimental analysis on the target DCT driveline, the certain gain crossover frequency is determined such that the corresponding bandwidth does not exceed the bandwidth limit of the actual hardware. A more complex loop shape can be adopted as the desired loop shape G_d to improve the closed-loop control performance, but it may increase the order of the resulting H-infinity controller markedly, which is not desirable. Here, a stable minimum phase prefilter W is derived using the greatest common divisor formula [41] such that the singular values of $G_s = WG$ are approximately identical to those of G_d in a finite frequency domain. To obtain the robust stabilizing feedback control, it is assumed that the nominal shaped plant G_s designed by the prefilter has normalized left coprime factorization as follows [40]:

$$G_s = M^{-1}N. \tag{10}$$

The perturbed shaped plant $G_{s,p}$ then can be represented as:

$$G_{s,p} = \left\{ (M+\Delta_M)^{-1}(N+\Delta_N) : \left\| \begin{bmatrix} \Delta_N & \Delta_M \end{bmatrix} \right\|_\infty < \varepsilon \right\}, \tag{11}$$

where Δ_M and Δ_M are stable unknown transfer functions representing the model uncertainties, $\| \cdot \|_\infty$ denotes the H-infinity norm, and $\varepsilon > 0$ is the stability margin. For the perturbed system with the feedback controller K_s, the stability property is robust if and only if the nominal feedback system is stable and

$$\gamma = \left\| \begin{bmatrix} K_s \\ I \end{bmatrix} (I - G_s K_s)^{-1} M^{-1} \right\|_\infty \le \frac{1}{\varepsilon}. \tag{12}$$

The optimal (lowest) value of γ and the maximum stability margin ε are provided as (13) [38].

$$\gamma_{\min} = \varepsilon_{\max}^{-1} = \left\{ 1 - \left\| \begin{bmatrix} N & M \end{bmatrix} \right\|_H^2 \right\}^{-\frac{1}{2}} = \left(1 + \rho(XZ)\right)^{\frac{1}{2}}, \tag{13}$$

where $\| \cdot \|_H^2$ is the Hankel norm and ρ is the spectral radius.

In (13), for the minimal state-space realization (A, B, C, D) of G_s, Z and X are the unique positive definite solutions to the following two algebraic Riccati equations (14) and (15).

$$\begin{aligned} &\left(A - BS^{-1}D^TC\right)Z + Z\left(A - BS^{-1}D^TC\right)^T \\ &-ZC^TR^{-1}CZ + BS^{-1}B^T = 0 \end{aligned} \tag{14}$$

where $R = I + DD^T$, $S = I + D^TD$ and

$$\begin{aligned} &\left(A - BS^{-1}D^TC\right)X + X\left(A - BS^{-1}D^TC\right)^T \\ &-XBR^{-1}B^TZ + C^TR^{-1}C = 0 \end{aligned} \tag{15}$$

Here, the shaped plant (11) for the DCT driveline has $D \approx 0$, and thus, equations (14) and (15) are significantly simplified. Then, the stabilizing controller K_s for G_s that guarantees

$$\left\| \begin{bmatrix} K_s \\ I \end{bmatrix} (I - G_s K_s)^{-1} M^{-1} \right\|_\infty \le \gamma \tag{16}$$

for a specified $\gamma > \gamma_{\min}$ is derived using the explicit formula specified in [39]. The final H-infinity loop shaping controller is denoted as $K = WK_s$. The singular values of the resulting closed-loop shape as well as the shaped plant by the prefilter are exhibited in Fig. 5. From the results of the multivariable control strategy, the closed-loop system exhibited decoupled and good tracking responses. The robust stability of the H-infinity controller will guarantee the desired control performance even in the presence of unknown disturbances.

3) Feedforward Control Law

In order to improve the transient response of the controller, one can increase the feedback gain or the gain crossover frequency of the designed prefilter. However, just increasing the feedback gain can easily cause undesirable oscillatory responses according to the driving circumstances. Thus, a feedforward control law for the clutch 2 input is derived to improve the torque tracking response, as follows:

$$T_{c2,FF} = f^{-1}\left(\dot{r}_2, r_2, x_2\right), \tag{17}$$

where the dynamics of the third state in (1) is denoted as:

$$\begin{aligned} \dot{y}_2 = \dot{x}_3 &= k_{o,eq}x_2 - c_{o,eq}\left(\frac{1}{i_{t2}i_{f2}J_{ct2,eq}} + \frac{1}{J_v}\right)x_3 \\ &+ \frac{1}{J_{ct2,eq}}T_{c2} + \frac{c_{o,eq}}{J_v}T_v = f\left(T_{c2}, x_2, x_3\right), \end{aligned} \tag{18}$$

In equation (18), the vehicle load torque is calculated using (3). To investigate the effects of the feedforward control on the whole control responses, several experiments were carried out for three controller types: feedback control (H-infinity loop shaping) only, feedforward control only, and a combination of them. The corresponding results are shown in Fig. 7.

The feedforward only case exhibited a fast response at the beginning but cannot track the desired value accurately due to the model uncertainties. Also, the results of the feedback control showed slow response at the beginning, and exhibited unwanted oscillatory responses to track the desired values. However, when using combined control of feedforward and feedback, the tracking performance was greatly improved since it took advantage of both the control laws.

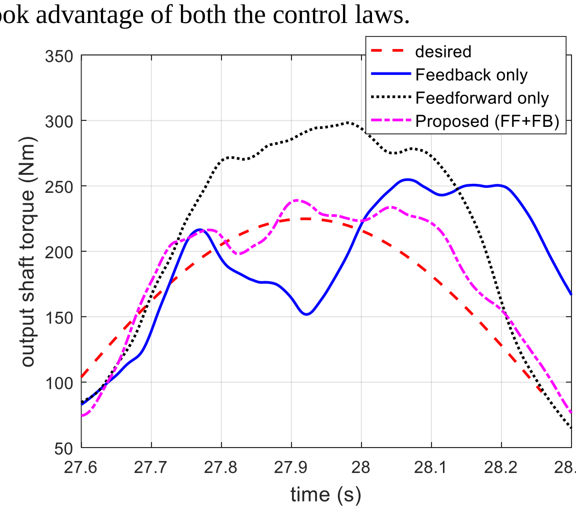

Fig. 7. Tracking performance comparison: (1) feedback control only (H-infinity loop shaping controller), (2) feedforward control only, (3) feedback + feedforward control (proposed)

The final controller is developed as the observer-based multivariable controller combined with the feedforward control, as described in Fig. 6.

E. End Phase Control

In order to treat the driveline oscillations effectively, an additional damping control law is designed for the end phase. A feedback control law aimed at reducing the difference of the transmission input speed (multiplied by gear ratios) and wheel speed is designed to attenuate the lock-up oscillations. Using the fast torque response of the drive motor, the driveline oscillations at the beginning of the end phase can be significantly improved. During the end phase, the stroke of the on-coming clutch should be increased further to ensure its lock-up.

IV. Experiments

A. Experimental Set-ups

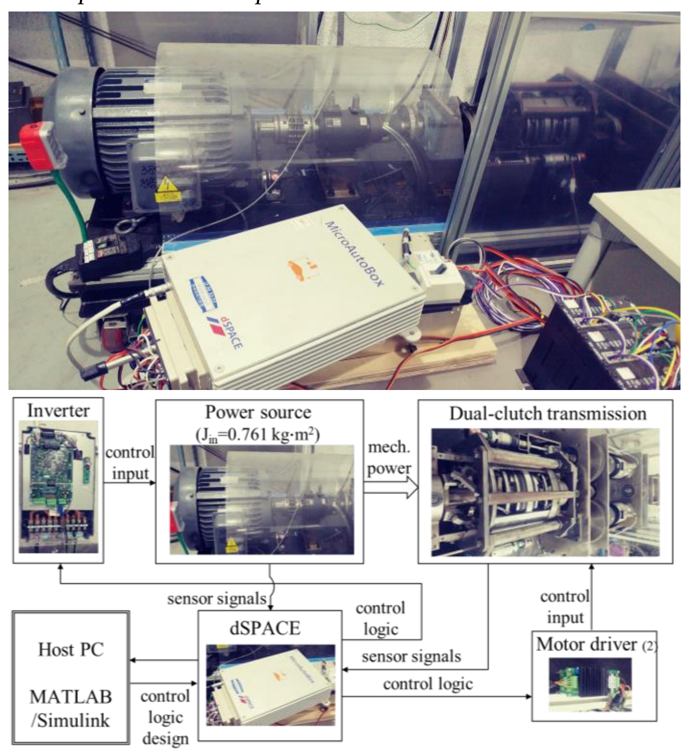

Fig. 8. Test-bench set-up for control validations

Fig. 8 describes the DCT test bench used for the experimental validations of the proposed algorithm. The system parameter values are presented in Table II. The mechanical structure of the bench is identical to that of production DCTs, and encoders were attached on several shafts to provide the speed data of the driveline to the controller. Also, torque transducers were mounted to the shafts additionally for validation purpose only. MicroAutobox dSPACE 1401 was used to process the signals from the sensors and to run the control algorithm in real-time. It is worth noting that this test-bench is suitable for testing the driveline control of a parallel HEV especially when it is operating in the parallel mode. The power source inertia is very large enough to represent the equivalent inertia of all the components in the power source side in a real car.

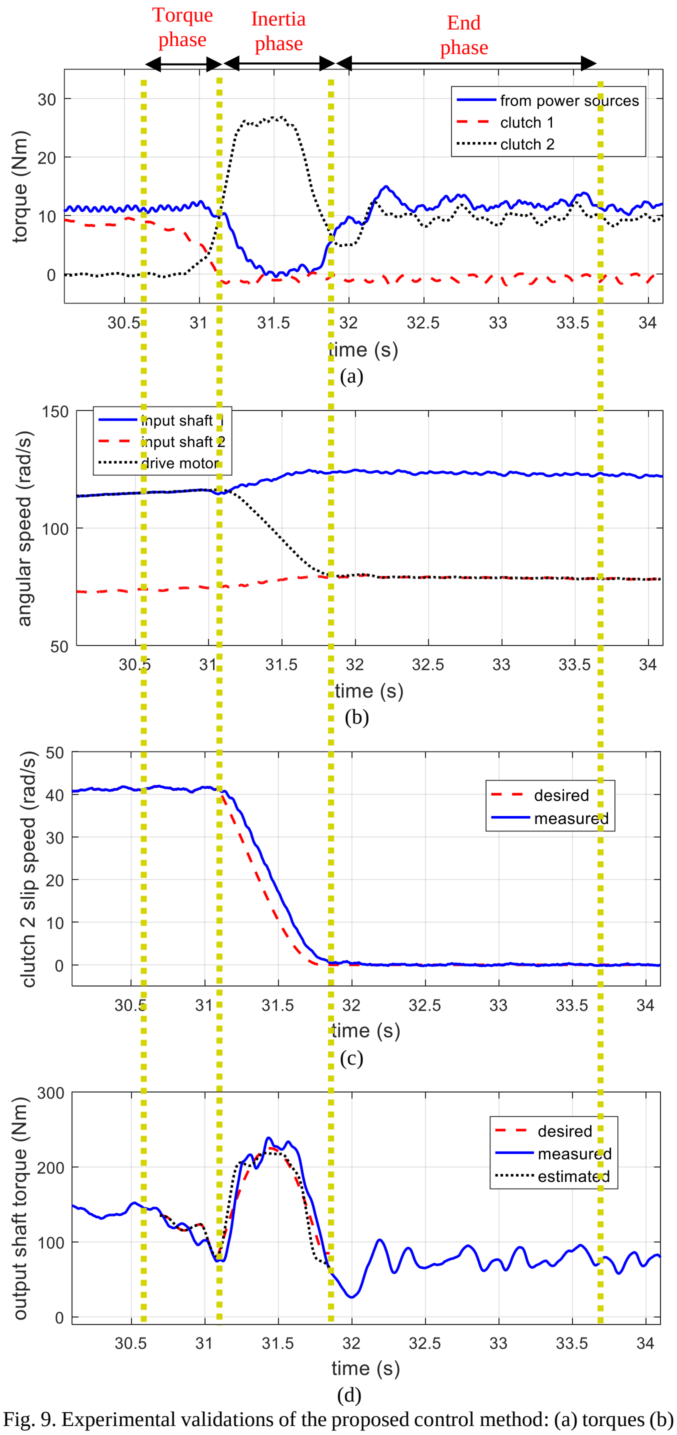

Fig. 9. Experimental validations of the proposed control method: (a) torques (b) angular speeds, (c) slip speed of on-coming clutch, (d) output shaft torque

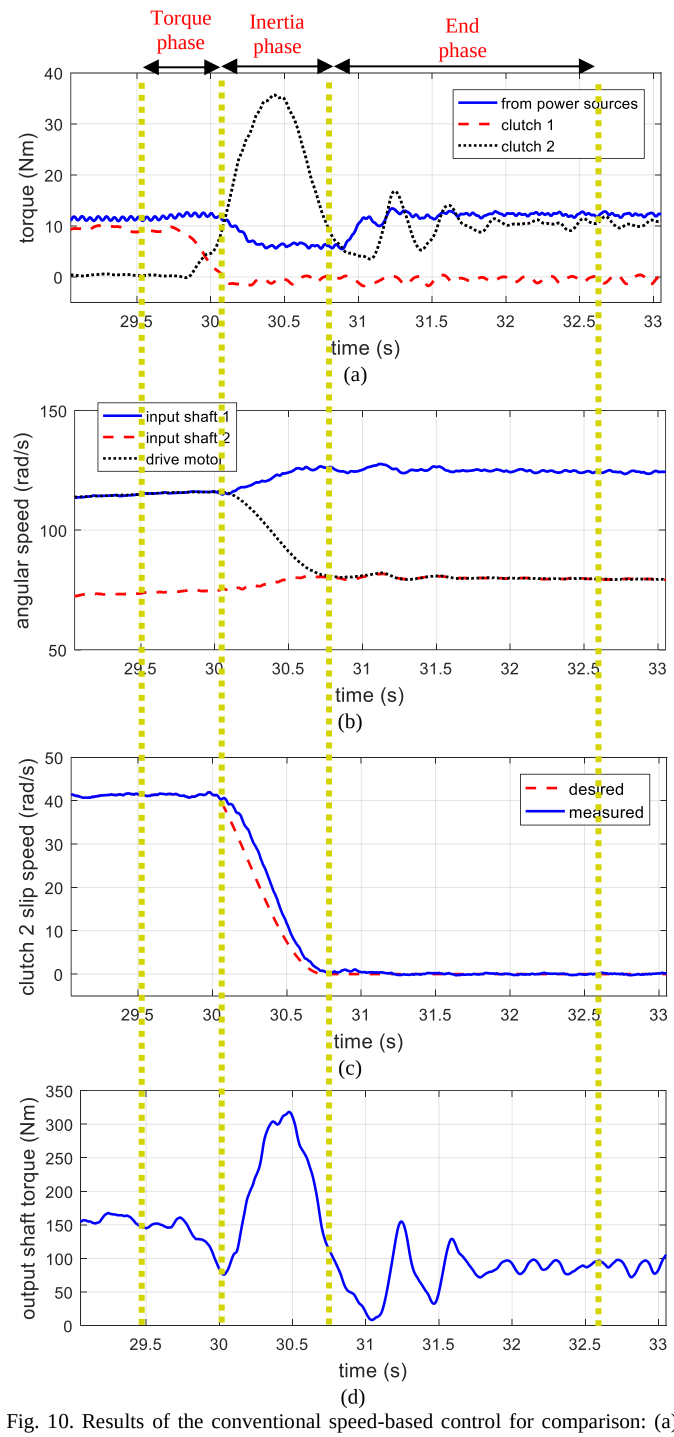

Fig. 10. Results of the conventional speed-based control for comparison: (a) torques (b) angular speeds, (c) slip speed of on-coming clutch, (d) output shaft torque

TABLE II

PARAMETERS FOR THE TEST-BENCH

Test-bench parameters	
$J_{in} = 0.761$	$k_o = 10000$
$J_{ct2,eq} = 3.97$	$c_o = 700$
$J_v = 135$	$i_{f1} = 6$
$i_{t1} = 3$	$i_{f2} = 4.8$
$i_{t2} = 2.4$	Units are SI derived. (kg, N, m, rad, s)

B. *Validations of the Proposed Control Strategy*

Experiments on the DCT test bench were carried out in order to validate the whole control scheme experimentally. The final control results are shown in Fig. 9. Since the proposed control strategy used the feedback control based on the dynamic torque observer, the estimated output torque is also plotted in Fig. 9(d). The slip speed and output shaft torque tracked the desired values in the inertia phase well to ensure the smooth and fast clutch engagement, so the lock-up oscillations were considerably reduced with the aid of the end phase control. Note that the magnitude of the desired output torque overshoot is designed to be somewhat large (Fig. 9(d)) because the inertia of power sources in this test-bench is quite large.

C. Comparison with the Conventional Method

Next, another experiment based on the conventional control method was also conducted for comparative studies, and the results are provided in Fig. 10. The conventional method was based merely on the slip speed feedback, which was implemented in the form of a decentralized structure. The objective of the speed-based controller was to track the desired slip speed trajectory accurately without considering other torque states.

In general, the magnitude of jerk or squared jerk itself represents the corresponding physical shock people can feel, but the shift time should also be considered when evaluating the ride quality during a gear shift. Thus, the integral value of squared vehicle jerk during inertia and end phases is considered in order to evaluate the shift shock quantitatively [42]. For an accurate comparison, the desired shift time was intentionally fixed for both cases (Figs. 9 and 10). Even though both results exhibited the same performance in terms of the shift time, the proposed approach exhibited much better ride quality performance during the gear shift, as shown in Table III. The conventional control strategy based only on speed information could not directly regulate the shift shock (large torque oscillation was observed in Fig. 10(d)), while the proposed control achieved the smooth shift by controlling the transient output torque in addition to the slip speed. In result, it was experimentally verified that the integrated speed and torque control approach is very effective for control of HEV with DCT.

TABLE III
QUANTITATIVE COMPARISON OF THE CONVENTIONAL AND PROPOSED CONTROLS

Control strategy	Shift time (s)	Integral of squared jerk (m/s^5)
Conventional	1.24	3.14
Proposed	1.24	1.53

V. CONCLUSION

This paper proposed an integrated torque and speed control strategy for gear shift processes of a parallel-type HEV with DCT. A HEV has a drive motor directly attached to the transmission so that it can be used for the shift control. Compared with the conventional engine-driven vehicles, there is notable possibility to improve the gear shift performance of the HEV using the fast dynamic characteristic and the regenerative operation of the drive motor. However, a HEV has significantly large inertias in its power source side, which may result in large oscillations in driveline during gear shifts, so sophisticated control of clutches and power sources is required when conducting a gear shift.

In this work, different control strategies were developed for the three phases of a gear shift process. For the inertia phase, in particular, a robust multivariable controller based on H-infinity loop shaping was designed to effectively control both clutch slip speed and output shaft torque. The reference trajectories of the states were delicately designed to satisfy the desired shifting performances, considering the conflict between the smooth and fast shifting conditions. An adaptive torque observer was developed to concurrently monitor the transmitted torque of both clutches and the output shaft in the driveline, which was used to improve the torque control performance of the proposed controller. The whole observer-based control scheme was validated using experiments on the test-bench. Comparative studies were also conducted to demonstrate the effectiveness of the propose control, and the results indicated that the proposed torque/speed control strategy significantly improved the shift performance of the HEV with DCT. Future works may include the development of a control strategy based on the dynamic torque observer for a downshift of vehicles with DCT.

ACKNOWLEDGMENT

This work was supported by the National Research Foundation of Korea grant funded by the Korea government (MSIP) (No.2017R1A2B4004116).

REFERENCES

[1] P. Pisu and G. Rizzoni, "A comparative study of supervisory control strategies for hybrid electric vehicles," *IEEE Transactions on Control Systems Technology,* vol. 15, pp. 506-518, 2007.

[2] D. Kum, H. Peng, and N. K. Bucknor, "Supervisory control of parallel hybrid electric vehicles for fuel and emission reduction," *Journal of dynamic systems, measurement, and control,* vol. 133, p. 061010, 2011.

[3] C.-C. Lin, H. Peng, J. W. Grizzle, and J.-M. Kang, "Power management strategy for a parallel hybrid electric truck," *IEEE transactions on control systems technology,* vol. 11, pp. 839-849, 2003.

[4] X. Zeng and J. Wang, "Optimizing the Energy Management Strategy for Plug-In Hybrid Electric Vehicles With Multiple Frequent Routes," *IEEE Transactions on Control Systems Technology,* 2017.

[5] Y. Wang, X. Wang, Y. Sun, and S. You, "Model predictive control strategy for energy optimization of series-parallel hybrid electric vehicle." Journal of Cleaner Production 199 (2018): 348-358.

[6] T. Liu, X. Hu, S. E. Li, and D. Cao, "Reinforcement Learning Optimized Look-Ahead Energy Management of a Parallel Hybrid Electric Vehicle," *IEEE/ASME Transactions on Mechatronics,* vol. 22, pp. 1497-1507, 2017.

[7] H. Wang, Y. Huang, and A. Khajepour, "Cyber-Physical Control for Energy Management of Off-road Vehicles with Hybrid Energy Storage Systems," *IEEE/ASME Transactions on Mechatronics,* 2018.

[8] P. Walker, B. Zhu, and N. Zhang, "Powertrain dynamics and control of a two speed dual clutch transmission for electric vehicles," *Mechanical Systems and Signal Processing,* vol. 85, pp. 1-15, 2017.

[9] Z. Lei, D. Sun, Y. Liu, D. Qin, Y. Zhang, Y. Yang, *et al.*, "Analysis and coordinated control of mode transition and shifting for a full hybrid electric vehicle based on dual clutch transmissions," *Mechanism and Machine Theory,* vol. 114, pp. 125-140, 2017.

[10] S. Hong, S. Ahn, B. Kim, H. Lee, and H. Kim, "Shift control of a 2-speed dual clutch transmission for electric vehicle," in *Vehicle Power and Propulsion Conference (VPPC), 2012 IEEE,* 2012, pp. 1202-1205.

[11] Z.-G. Zhao, H.-J. Chen, Y.-Y. Yang, and L. He, "Torque coordinating robust control of shifting process for dry dual clutch transmission equipped in a hybrid car," *Vehicle System Dynamics,* vol. 53, pp. 1269-1295, 2015.

[12] E. Galvagno, M. Velardocchia, and A. Vigliani, "Dynamic and kinematic model of a dual clutch transmission," *Mechanism and Machine Theory,* vol. 46, pp. 794-805, 2011.

[13] J. Kim, S. B. Choi, and J. J. Oh, "Adaptive Engagement Control of a Self-Energizing Clutch Actuator System Based on Robust Position Tracking," *IEEE/ASME Transactions on Mechatronics,* vol. 23, pp. 800-810, 2018.

[14] Y. Liu, D. Qin, H. Jiang, and Y. Zhang, "Shift control strategy and experimental validation for dry dual clutch transmissions," *Mechanism and Machine Theory,* vol. 75, pp. 41-53, 2014.

[15] K. van Berkel, T. Hofman, A. Serrarens, and M. Steinbuch, "Fast and smooth clutch engagement control for dual-clutch transmissions," *Control Engineering Practice,* vol. 22, pp. 57-68, 2014.

[16] X. Wang, L. Li, K. He, C. Liu, " Dual-Loop Self-Learning Fuzzy Control for AMT Gear Engagement: Design and Experiment," IEEE Transactions on Fuzzy Systems, Vol. 26, pp.1813-1822, 2017.

[17] B. Z. Gao, H. Chen, K. Sanada, and Y. Hu, "Design of clutch-slip controller for automatic transmission using backstepping," *Mechatronics, IEEE/ASME Transactions on,* vol. 16, pp. 498-508, 2011.

[18] F. Meng, G. Tao, T. Zhang, Y. Hu, and P. Geng, "Optimal shifting control strategy in inertia phase of an automatic transmission for automotive applications," *Mechanical Systems and Signal Processing,* vol. 60, pp. 742-752, 2015.

[19] F. Liu, L. Chen, D. Li, and C. Yin, "Improved clutch slip control for automated transmissions," *Proceedings of the Institution of Mechanical Engineers, Part C: Journal of Mechanical Engineering Science,* p. 0954406217734578, 2017.

[20] P. D. Walker, N. Zhang, and R. Tamba, "Control of gear shifts in dual clutch transmission powertrains," *Mechanical Systems and Signal Processing,* vol. 25, pp. 1923-1936, 2011.

[21] M. Goetz, M. Levesley, and D. Crolla, "Dynamics and control of gearshifts on twin-clutch transmissions," *Proceedings of the institution of mechanical engineers, Part D: Journal of Automobile Engineering,* vol. 219, pp. 951-963, 2005.

[22] S. Kim, J. Oh, and S. Choi, "Gear shift control of a dual-clutch transmission using optimal control allocation," *Mechanism and Machine Theory,* vol. 113, pp. 109-125, 2017.

[23] S. Kim, J. J. Oh, and S. B. Choi, "Driveline Torque Estimations for a Ground Vehicle with Dual-clutch Transmission," *IEEE Transactions on Vehicular Technology,* vol. 67, pp. 1977-1989, 2018.

[24] Z. Zhao, L. He, Y. Yang, C. Wu, X. Li, and J. K. Hedrick, "Estimation of torque transmitted by clutch during shifting process for dry dual clutch transmission," *Mechanical Systems and Signal Processing,* vol. 75, pp. 413-433, 2016.

[25] Z. Zhao, X. Li, L. He, C. Wu, and J. K. Hedrick, "Estimation of Torques Transmitted by Twin-clutch of Dry Dual Clutch Transmission during Vehicle's Launching Process," *IEEE Transactions on Vehicular Technology,* 2016.

[26] J. Oh, S. Choi, Y. Chang, and J. Eo, "Engine clutch torque estimation for parallel-type hybrid electric vehicles," *International Journal of Automotive Technology,* vol. 18, pp. 125-135, 2017.

[27] M. Song, J. Oh, S. Choi, Y. Kim, and H. Kim, "Motor control of a parallel hybrid electric vehicle during mode change without an integrated starter generator," *Journal of Electrical Engineering & Technology (JEET),* vol. 8, pp. 930-937, 2013.

[28] A. Myklebust and L. Eriksson, "Modeling, observability, and estimation of thermal effects and aging on transmitted torque in a heavy duty truck with a dry clutch," IEEE/ASME transactions on mechatronics, vol. 20, pp. 61-72, 2015.

[29] M. Pisaturo, A. Senatore, "Simulation of engagement control in automotive dry-clutch and temperature field analysis through finite element model," Applied Thermal Engineering, vol. 93, pp.958-966, 2016.

[30] M. Pisaturo, A. Senatore, and V. D'Agostino, "Automotive dry-clutch control: Engagement tracking and FE thermal model," Proceedings of IEEE 20th Jubilee International Conference on Intelligent Engineering Systems, 2016.

[31] A. D. Gatta, L. Iannelli, M. Pisaturo, A. Senatore and F. Vasca, "A Dry Clutch Engagement Controller with Thermal Effects Compensation," Proceedings of 2018 IEEE Conference on Control Technology and Applications, Copenhagen, pp. 1228-1233, 2018.

[32] S. Kim and S. Choi, "Control-oriented modeling and torque estimations for vehicle driveline with dual-clutch transmission," *Mechanism and Machine Theory,* vol. 121, pp. 633-649, 2018.

[33] Z. Zhao, D. Lei, J. Chen, and H. Li, "Optimal control of mode transition for four-wheel-drive hybrid electric vehicle with dry dual-clutch transmission," *Mechanical Systems and Signal Processing,* vol. 105, pp. 68-89, 2018.

[34] V. Ranogajec and J. Deur, "Bond graph analysis and optimal control of the hybrid dual clutch transmission shift process," *Proceedings of the Institution of Mechanical Engineers, Part K: Journal of Multi-body Dynamics,* vol. 231, pp. 480-492, 2017.

[35] B. Gao, H. Chen, J. Li, L. Tian, and K. Sanada, "Observer-based feedback control during torque phase of clutch-to-clutch shift process," *International Journal of Vehicle Design,* vol. 58, pp. 93-108, 2012.

[36] M. Pettersson and L. Nielsen, "Gear shifting by engine control," *IEEE Transactions on Control Systems Technology,* vol. 8, pp. 495-507, 2000.

[37] F. Garofalo, L. Glielmo, L. Iannelli, and F. Vasca, "Smooth engagement for automotive dry clutch," in *Decision and Control, 2001. Proceedings of the 40th IEEE Conference on,* 2001, pp. 529-534.

[38] D. McFarlane and K. Glover, "A loop-shaping design procedure using H/sub infinity/synthesis," *IEEE transactions on automatic control,* vol. 37, pp. 759-769, 1992.

[39] K. Glover and D. McFarlane, "Robust stabilization of normalized coprime factor plant descriptions with H/sub infinity/-bounded uncertainty," *IEEE transactions on automatic control,* vol. 34, pp. 821-830, 1989.

[40] S. Skogestad and I. Postlethwaite, *Multivariable feedback control: analysis and design* vol. 2: Wiley New York, 2007.

[41] V. Le and M. Safonov, "Rational matrix GCDs and the design of squaring-down compensators-a state-space theory," *IEEE Transactions on Automatic Control,* vol. 37, pp. 384-392, 1992.

[42] J. Levinson, J. Askeland, J. Becker, J. Dolson, D. Held, S. Kammel, *et al.,* "Towards fully autonomous driving: Systems and algorithms," in *Intelligent Vehicles Symposium (IV), 2011 IEEE,* 2011, pp. 163-168.

Sooyoung Kim received his B.S. and M.S. degrees, and Ph.D. in mechanical engineering from KAIST, Daejeon, Korea.

He is currently a Senior Research Engineer with Hyundai Motor Company, Hwasung, South Korea. His current research interests include model-based control and state estimation of powertrains for mass-produced vehicles.

Seibum B. Choi (M'09) received his B.S. in mechanical engineering from Seoul National University, Seoul, Korea, his M.S. in mechanical engineering from KAIST, Daejeon, Korea, and his Ph.D. in control from the University of California, Berkeley, CA, USA, in 1993.

From 1993 to 1997, he was involved in the development of automated vehicle control systems at the Institute of Transportation Studies, University of California. Through 2006, he was with TRW, Livonia, MI, USA, where he was involved in the development of advanced vehicle control systems. Since 2006, he has been faculty in the Mechanical Engineering Department, KAIST, Korea. His current research interests include fuel-saving technology, vehicle dynamics and control, and active safety systems.

Prof. Choi is a Member of the American Society of Mechanical Engineers, the Society of Automotive Engineers, and the Korean Society of Automotive Engineers.